

# The GZK horizon and constraints on the cosmic ray source spectrum from observations in the GZK regime

M. Kachelrie<sup>1</sup>, E. Parizot<sup>2</sup>, and D. V. Semikoz<sup>2,3,4</sup>

<sup>1</sup> Institutt for fysikk, NTNU, N-7491 Trondheim, Norway

<sup>2</sup> APC, 10, rue Alice Domon et Leonie Duquet, F-75205 Paris Cedex 13, France

<sup>3</sup> CERN Theory Division, CH-1211 Geneva 23, Switzerland

<sup>4</sup> INR RAS, 60th October Anniversary prospect 7a, 117312 Moscow, Russia

We discuss the GZK horizon of protons and present a method to constrain the injection spectrum of ultrahigh energy cosmic rays (UHECRs) from supposedly identified extragalactic sources. This method can be applied even when only one or two events per source are observed and is based on the analysis of the probability for a given source to populate different energy bins, depending on the actual CR injection spectral index. In particular, we show that for a typical source density of  $4 \cdot 10^{-5} \text{ Mpc}^{-3}$ , a data set of 100 events above  $6 \cdot 10^{19} \text{ eV}$  allows one in 97% of all cases to distinguish a source spectrum  $dN=dE/E^{-1.1}$  from one with  $E^{-2.7}$  at 95% confidence level.

PACS: 98.70.Sa

Introduction| One of the main obstacles to fast progress in cosmic ray (CR) physics has been the impossibility to identify individual sources. However, there are two pieces of evidence indicating that we are at the dawn of "charged particle astronomy." First, anisotropies on medium scales have been found combining all available data of "old" CR experiments [1] as well as in the data from the Pierre Auger Observatory (Auger) [2]. Second, the Auger data hint for a correlation of UHECRs and active galactic nuclei (AGN) [3], although this correlation has been contested [4]. Thus one may anticipate that the influence of extragalactic magnetic fields is small so that UHECRs are not significantly deflected from their initial direction. This should be particularly true above the GZK cutoff at  $5 \cdot 10^{19} \text{ eV}$ , when the range of UHECRs is significantly reduced by their interactions with photons from the cosmic microwave background (CMB). For instance, for typical energy spectra and sources distributed roughly homogeneously throughout the universe, 70% of the protons with an observed energy of  $80 \text{ EeV}$  come from sources closer than  $100 \text{ Mpc}$ , even accounting for a 20% error in the energy determination. Over such distances, the angular spread caused by random magnetic fields of  $1 \text{ nG}$  is typically  $< 3^\circ$  for such high-energy protons. Deflections in the Galactic magnetic field are expected to be of the same order of magnitude [6].

The main reason why no sources have been identified yet would be in this scenario that the accumulated sky exposure is not yet large enough. While larger exposures will inevitably increase the number of UHECRs detected per source, it may take many years until

enough events are accumulated from even the most intense source in the sky to allow one drawing a decent individual spectrum. The diffuse energy spectrum of CRs below  $E < 4 \cdot 10^{19} \text{ eV}$  is known with reasonable accuracy and requires a generation spectrum  $dN=dE/E^{-2.7}$  with  $\pm 0.1$  for identical sources or an appropriate distribution of maximal energies  $E_{\text{max}}$  [7] while both the source and the diffuse spectra at higher energies are essentially unknown. It is therefore timely, in the intermediate phase when sources may be identified by correlation studies but typically only one or two events per source are detected, to ask how the injection spectrum can be determined best.

While first-order Fermi shock acceleration typically results in  $\gamma$  around 2.1 [8], there exist various models that predict either much harder or softer spectra. An example for a model with  $\gamma$  up to  $10^{20} \text{ eV}$  is the acceleration in the electric field around supermassive black holes suggested in Ref. [9, 10] that explains also the observed properties of large scale jets in AGN [11]. Another possibility to obtain  $\gamma$  is to take into account a large photon background in the acceleration region in the usual shock acceleration [12]. On the other hand, pinch acceleration may serve as an example for  $\gamma = 2.7$  [13].

In this work, we present an alternative method to set constraints on the UHECR source spectrum, suitable for the near future of proton astronomy. The basic idea to constrain the spectral index of individual sources is that, even though the relative weight of different sources cannot be known in advance (i.e. before measuring their spectra individually), the relative weight of different en-

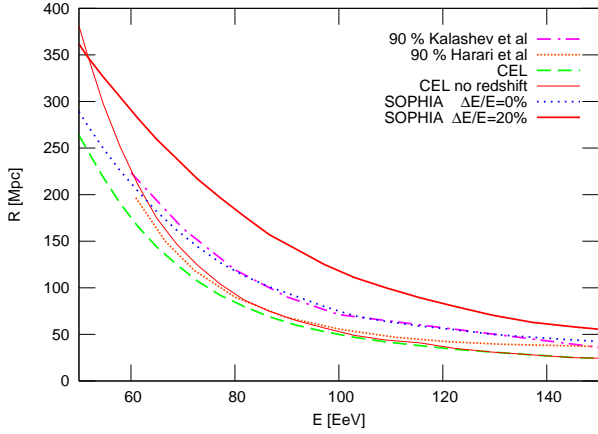


Fig. 1: Distance  $R$  in Mpc from which 90% of UHECRs arrive with energy  $> E$  as function of the threshold energy  $E$  for  $E_{\text{max}} = 10^{21}$  eV and  $\beta = 2.7$ . The thin solid red line uses CEL in a static Universe as [19], the green line uses CEL in an expanding Universe. The blue line labeled "SOPHIA" has to be compared to [20]. The red line takes into account additionally an experimental energy resolution  $\Delta E/E = 20\%$ .

energy bins for a given source is a direct consequence of the source spectrum. Now suppose that a minimal energy  $E_{\text{min}}$  can be identified, above which we can trust that the observed CRs come roughly in straight lines from their source and, most importantly, sources inside the horizon appear with a small enough angular spread on the sky that they do not overlap. The energy distribution of CRs seen above  $E_{\text{min}}$  from a given source should then reflect the source spectrum (modified by the usual propagation effects), and even if one observes only one of them, its energy contains some information about the source spectrum. We show how this simple argument can be implemented quantitatively for a given data set, taking into account UHECR energy losses from pure proton sources with supposedly identified distances and identical maximum energy. We use this toy model to illustrate the basic features of the method and to explore its potential power, leaving necessary refinements for future work.

Propagation and horizon scale of UHE protons | In Fig. 1, we show the "90% horizon" (i.e. the distance  $R_{90}$  from which 90% of the UHECRs observed above a given energy,  $E$ , originate) as function of energy. We assume a uniform source distribution with a density  $n_s = 4 \cdot 10^5 \text{ Mpc}^3$  (cf. e.g. Refs. [14, 15]) and a power-law source spectrum  $dN = dE / E^\beta$  with  $\beta = 2.7$  up to the maximal energy  $E_{\text{max}} = 10^{21}$  eV. We used for the calculation of photo-pion production the program SOPHIA [16], either taking into account the stochastic-

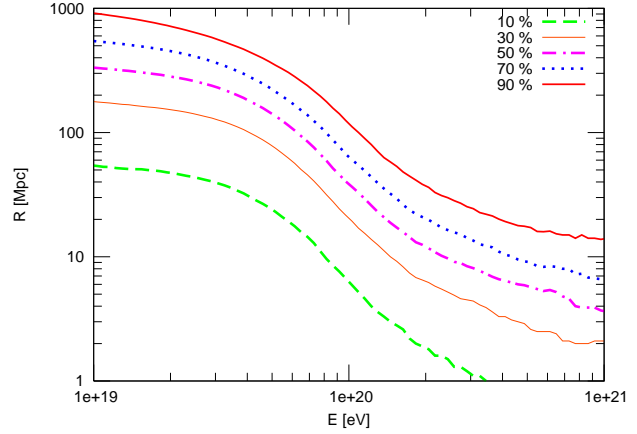


Fig. 2: The distance  $R$  in Mpc for which a certain fraction  $f$  of UHECRs arrives with energy  $> E$  as function of the energy threshold  $E$  for  $\beta = 2.7$ . From top to bottom,  $f = 90\%$  as red line,  $f = 70\%$  as pink,  $f = 50\%$  as magenta,  $f = 30\%$  as blue and  $f = 10\%$  as green line.

ity of the corresponding energy losses (dotted, blue line) or applying the continuous energy loss (CEL) approximation to its results (dashed, green line). The  $e^+e^-$  pair production losses were taken from Ref. [17].

The  $f = 90\%$  horizon computed within the CEL approximation underestimates considerably the full Monte Carlo result. The difference increases for a larger "horizon fraction",  $f \neq 1$ , and as function of energy for  $E \neq E_{\text{max}}$ . There are two reasons for the latter discrepancy. First, the energy transfer per interaction,  $y$ , increases with energy and violates more and more strongly the formal requirement  $y \leq 1$  needed for the applicability of the CEL approximation. Second, the flux taking into account the stochastic nature of the energy losses in pion production remains finite for  $E \neq E_{\text{max}}$ , while in the CEL approximation no particles with  $E = E_{\text{max}}$  can reach the observer from a source at a finite distance [8].

In a realistic experiment, the primary energy can only be reconstructed with a finite precision. Assuming a Gaussian (in  $\log E$ ) experimental uncertainty of  $\Delta E/E = 20\%$ , we computed the 90% horizon as a function of the measured CR energy, for the same conditions as above. The two resulting curves are also shown in Fig. 1. Since the CR spectrum is falling steeply, the misinterpretation of lower energy events as high energy ones has a larger impact than the reverse, which in turn leads to an increase of the estimated horizon scale. At low energies, say  $< 5 \cdot 10^9$  eV, the observed spectrum approximates well to a power-law and the energy resolution only affects the absolute flux, not the relative fluxes relevant for  $R_{90}(E)$ .

The horizon scale for UHE protons and nuclei was recently discussed also in Refs. [19, 20]. In Fig. 1 we compare our calculations to those of Refs. [19] and [20] for proton primaries. In Ref. [19], Harari et al. presented results (shown as orange line) using the CEL approximation and assuming a static Universe, our result for the same assumptions is shown with a thin solid red line. Both calculations agree well at moderate energies  $E = 80 - 100 \text{ EeV}$ , while there is some disagreement both at high and low energies. However, the differences at low energies between the two calculations are much smaller than the differences between those calculations and the more correct CEL calculation in the  $\Lambda$ CDM model for the expanding Universe, presented with a green line.

All results using the CEL approximation differ in shape as a function of energy from the calculations using SOPHIA for pion production either directly (blue line), or using the SOPHIA results in a kinetic equation approach as in Ref. [20] (magenta line). The agreement between the latter two results is almost perfect at all energies.

As an illustration, we show in Fig. 2 the horizon distance corresponding to different CR fractions. Specifically, we plot the distance  $R_f$  below which a given fraction  $f$  of the UHECRs reach the Earth with an energy larger than  $E$ , as a function of that energy, for  $f = 10\%$ ,  $30\%$ ,  $50\%$ ,  $70\%$  and  $90\%$  (using always SOPHIA and  $E = E = 20\%$ ).

Estimation of the spectral index | Since the angular resolution of cosmic ray experiments is poor by astronomical standards, the identification of individual sources requires a relatively large angular distance between them. This can only hold for sufficiently high energies such that the horizon scale is small, say of the order of  $100 \text{ Mpc}$ , leaving a limited number of sources over the sky. Defining as horizon, within which  $90\%$  of all CRs observed above a given energy were emitted, we

find from Fig. 2 that a horizon of  $100 \text{ Mpc}$  corresponds to a threshold energy of  $E = 1 - 10^{20} \text{ eV}$ . At present, the importance of deflections in extragalactic magnetic fields above this energy is unclear. As soon as sources are detected, one will be able to set an upper limit and to a certain extent reconstruct the extragalactic magnetic field. Here, we limit ourselves to the optimistic scenario where deflections in extragalactic magnetic fields are not much larger than the combined effects of the Galactic magnetic field and the experimental angular resolution.

At present, the picture of uniformly distributed, extragalactic UHECR sources having all the same luminosity and the same injection spectrum is able to describe well the observed energy spectrum in a broad

energy range from a few  $10^{17} \text{ eV}$  or a few  $10^{18} \text{ eV}$  up to the GZK cutoff, depending on the assumed source composition [21, 22].

We first produce a Monte Carlo (MC) sample by generating sources with constant comoving density  $n_s = 4 - 10^5 \text{ Mpc}^{-3}$  up to a maximal redshift of  $z = 0.1$ . Then we choose a source  $i$  according to the declination dependent exposure of Auger, with an additional weight chosen according to the source distance. Finally, we generate a CR with an initial energy drawn randomly according to the assumed injection spectrum,  $dN = dE / E^{-\alpha}$ , and propagate it until it either reaches the Earth distance or loses energy down to below  $E_{\text{min}}$ . In the former case, we then apply an energy-dependent angular deflection to mimic the effect of the Galactic magnetic field, with a shift perpendicular to the Galactic plane equal to  $b = 2 (E = 10^{20} \text{ eV})^{-1}$ , where this magnitude is motivated by the results of Ref. [6]. The chosen magnetic field likely overestimates deflections far away from the galactic plane in most of models. However, we consider this choice as a conservative upper limit. Finally, we deflect the CR direction to account for a finite experimental angular resolution, taking the Auger surface detector as a reference [23], with a spherical Gaussian density  $\propto \exp(-\theta^2 = (2 \frac{\theta}{\theta_1})^2) \sin(\theta) d\theta$ , where  $\theta_1 = 0.85^\circ$  and  $\theta$  is the angular distance.

After having generated  $N$  cosmic rays, we perform a correlation analysis between the CRs and the sources. First, we identify as "the source" of a given CR the source with the smallest angular distance  $\theta$  to the observed CR arrival direction and maximal distance  $R = 100 \text{ Mpc}$ . Inside this region, there are around  $\sim 160$  sources for chosen density  $n_s = 4 - 10^5 \text{ Mpc}^{-3}$ . Such a small number makes the probability negligible that sources overlap, if they are uniformly distributed. This probability increases, if sources follow as expected the large-scale structure of matter and may constitute a real limitation to resolve single sources in cluster cores.

Additionally, we require that the angular distance  $\theta$  be smaller than a prescribed value,  $\theta_{\text{max}}$ . Next, having predefined an energy  $E_2$  that divides the whole energy range into two large bins, we count for each source  $i$  the numbers  $N_{i,1}$  and  $N_{i,2}$  of high energy ( $E > E_2$ ) and low energy events ( $E_{\text{min}} < E < E_2$ ), respectively. Given the corresponding fractions  $f_1(\theta)$  and  $f_2(\theta) = 1 - f_1(\theta)$  of  $N_i = N_{i,1} + N_{i,2}$  events expected from a source at the identified distance for an arbitrary value of the spectral index  $\alpha$ , we calculate with a binomial distribution the probability,

$$P_i(N_{i,1}; N_{i,2} | j) = \frac{(N_{i,1} + N_{i,2})!}{N_{i,1}! N_{i,2}!} f_1^{N_{i,1}}(\theta) f_2^{N_{i,2}}(\theta); \quad (1)$$

that the observed numbers  $N_{i,j}$  are consistent with the value  $\alpha_0$  used in the M.C. Considered as a function of  $\alpha$ , this probability distribution has the true value  $\alpha_0$  as its expectation value, if our procedure is unbiased, and measures how strongly the data disfavor a differently assumed value  $\alpha \neq \alpha_0$ .

Since the different sources emit CRs independently from one another, we can simply multiply the single source probabilities  $p_i(N_{i,1}; N_{i,2} | j)$  to obtain the global probability of a given data set with  $N_s$  identified sources:

$$p(\{N_{i,1}; N_{i,2} | j\}) = \prod_{i=1}^{N_s} p_i(f_{i,1}; f_{i,2} | j): \quad (2)$$

The basic outcome of a sample of MC simulations for fixed parameters  $\alpha = \alpha_0$  is thus a binned distribution,  $f(p, j)$ , giving the fraction  $f$  of MCs producing the value  $p$ . With how much confidence can we distinguish these distributions for two different  $\alpha_1$  and  $\alpha_2$ ? Clearly, the smaller the overlap of the two distributions, the easier the two parameter sets  $\alpha_i$  can be distinguished.

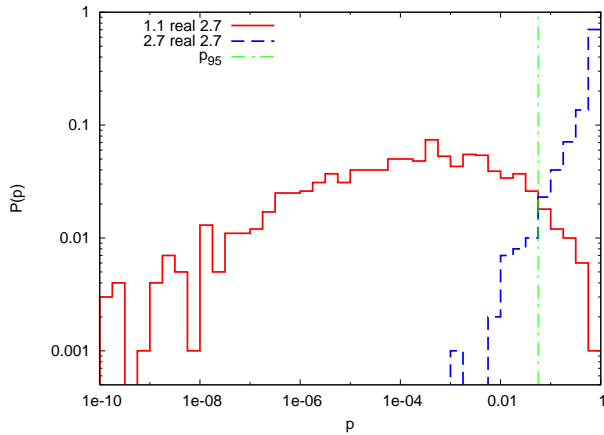


Fig. 3: Distribution of probability of reconstructed power law spectrum if real power law spectrum is  $\alpha = 2.7$ , angle  $\alpha'_{max} = 4$ . In all cases  $E_{min} = 60$  EeV. The red line is for  $\alpha = 1.1$  and the blue line for  $\alpha = 2.7$ .

We study now the possibility to distinguish different values of the injection spectrum of CRs in more detail. As simplifying assumption we assume that the injection spectrum of all sources is the same, i.e. in particular that the maximal energy of all sources is identical. This assumption allows us to study the spectra only above  $4 \cdot 10^9$  eV, because at lower energies a spectral index  $\alpha < 2.6$  requires either additional Galactic sources or a non-uniform source distribution. In the latter case, either the source density or the luminosity of single sources should increase as function of redshift,  $n(z) = n_0(1+z)^m$  and  $L(z) = L_0(1+z)^n$  respec-

tively, or the maximal energy of sources is distributed as  $dn = dE_{max} / E_{max}^{3.6}$  [7]. Moreover, we consider only two extreme cases, namely a power-law with  $\alpha = 1.1$  and  $\alpha = 2.7$ .

In Fig. 3 we compare the distributions of probabilities obtained from Eq. (2) choosing as true value  $\alpha_0 = 2.7$ , as source density as always  $n_s = 4 \cdot 10^5 \text{ Mpc}^3$ , as number of CRs  $N = 100$ , and  $\alpha'_{max} = 4$ . The red solid line is the distribution of probabilities obtained assuming  $\alpha = 1.1$ , while the blue dashed line corresponds to  $\alpha = 2.7$ . The two curves have only a small overlap, since the probabilities using the correct  $\alpha$  are rather narrowly concentrated around  $p = 1$ , while the probability distribution using the wrong  $\alpha$  extends from extremely low values up to one. Thus an experimental differentiation between different injection spectra seems possible, even if only one or, in few cases, two events per source are detected, as it is the case for the chosen parameters in Fig. 3. This constitutes the main result of our work.

We quantify the chances to distinguish two different spectral indices in the following way: We calculate the area  $A$  corresponding to the desired confidence level (C.L.),  $A$ , starting from 1 to the left using the best-fit distribution (e.g. the blue line in Fig. 3) and obtain thereby as its lower boundary  $p_A$ . Thus only in  $1 - p_A$  cases we will obtain by chance a lower probability using the correct test hypothesis. Next we count how large is the area  $B$  of the wrong test hypothesis on the left of  $p_A$ . As final answer we obtain that in the fraction  $B$  of all cases we can distinguish between the two hypotheses with C.L.  $A$ .

Let us illustrate this procedure for the case considered above, choosing as confidence level  $A = 95\%$ . The green dashed-dotted vertical line in Fig. 3 enclosing 95% of the area of the true (blue) distribution determines  $p_{95} = 0.056$ . The area of the red curve on the left of  $p_{95} = 0.056$  is  $B = 0.971$ . Hence one can exclude in  $B = 97.1\%$  of cases with at least 95% C.L. the exponent  $\alpha = 1.1$  for the spectrum, if the true exponent is  $\alpha = 2.7$ .

In addition to the rather extreme cases of the spectral indices above, we investigated the ability of the method to distinguish between any of them and an intermediate value of  $\alpha = 2.0$ , often considered in the context of astrophysical particle acceleration. As an illustration, we found that with a data set of 100 cosmic rays above  $6 \cdot 10^9$  eV, it is possible in 50% of the cases to discriminate  $\alpha = 2.0$  from a value of either 1.1 or 2.7 with a C.L. of 95%. Likewise, for a data set of 200 cosmic rays above  $4 \cdot 10^9$  eV (i.e. for essentially the same exposure of the sky, but with a lower energy threshold), an injection spectral index of 1.1 can be discriminated

against  $\alpha = 2.0$  with a C.L. of 95% in 90% of the cases, while an injection spectral index of 2.7 can be discriminated against  $\alpha = 2.0$  with a C.L. of 95% in 70% of the cases.

**Summary** We have proposed a method to estimate the generation spectrum of individual extragalactic CR sources that is well-suited for the time when only one or two events per source are detected. An important ingredient of this method is the relative fraction of events contained in a prescribed energy interval. Therefore we have recalculated the horizon scale of ultra-high energy protons, taking into account a reasonable energy resolution, similar to that of Auger.

We have demonstrated for a toy model the potential of this method, finding that around 100 events above  $6 \cdot 10^9$  eV are required to distinguish with 97% probability at least at the 95% C.L. the two extreme cases  $\alpha = 1.1$  and 2.7. A differentiation between  $\alpha$ 's that are more similar will be clearly more challenging. An injection spectral index of 2.0 can still be distinguished from the two above values with a 95% C.L. in the majority of cases (with the same statistics).

Several of the issues we have neglected, like the effect of a possible  $E_{\text{max}}$  distribution, should be included in a more complete study as soon as experimental data will be available. A proper estimation of  $\alpha$  also requires to quantify the bias introduced e.g. by misidentified events. In general, it proves more efficient to remove from the data set the doubtful events (e.g. in regions where a given catalogue used to identify sources is known to be incomplete, or when several sources at different distances are identified over a small region of the sky, with possible overlap due to magnetic deflection or poor angular resolution), and apply the method with a correspondingly smaller statistics. Sources physically clustered in the universe are not a problem here, since they are located essentially at the same distance from the Earth and thus suffer from the same attenuation during propagation.

#### REFERENCES

1. M. Kachelrie and D. V. Semikoz, *Astropart. Phys.* 26, 10 (2006) [astro-ph/0512498].
2. S. Mollerach et al., to appear in *Proc. Mexico, 2007*, arXiv:0706.1749 [astro-ph].
3. J. Abraham et al. *Astropart. Phys.* 29, 188 (2008) [astro-ph/0712.2843].
4. R. U. Abbasi et al. [HiRes Collaboration], arXiv:0804.0382 [astro-ph]; D. S. Gorbunov et al., arXiv:0804.1088 [astro-ph]; I. V. Moskalenko et al., arXiv:0805.1260 [astro-ph].
5. K. Greisen, *Phys. Rev. Lett.* 16, 748 (1966); G. T. Zatsepin and V. A. Kuzmin, *JETP Lett.* 4, 78 (1966) [*Pisma Zh. Eksp. Teor. Fiz.* 4, 114 (1966)].
6. M. Kachelrie, P. D. Serpico and M. Teshima, *Astropart. Phys.* 26, 378 (2006) [astro-ph/0510444].
7. M. Kachelrie and D. V. Semikoz, *Phys. Lett. B* 634, 143 (2006) [astro-ph/0510188].
8. V. S. Berezinskii et al., *Astrophysics of cosmic rays*, Amsterdam: North-Holland 1990. T. Gaisser, *Cosmic Rays and Particle Physics*, Cambridge University Press 1991. R. J. Protheroe and R. W. Clayton, *Publ. Astron. Soc. of Australia* 21, 1 (2004) [astro-ph/0311466].
9. A. Neronov and D. Semikoz, *New Astronomy Review* s, 47, 693 (2003), A. Neronov, D. Semikoz and I. Tkachev, arXiv:0712.1737 [astro-ph].
10. A. Neronov, P. Tinyakov and I. Tkachev, *J. Exp. Theor. Phys.* 100, 656 (2005) [*Zh. Eksp. Teor. Fiz.* 100, 744 (2005)] [astro-ph/0402132].
11. A. Neronov, D. Semikoz, F. Aharonian and O. Kalashev, *Phys. Rev. Lett.* 89, 051101 (2002) [astro-ph/0201410].
12. E. V. Derishev et al., *Phys. Rev. D* 68, 043003 (2003) [astro-ph/0301263].
13. V. V. Vlasov, S. K. Zhdanov and B. A. Trubnikov, *Fiz. Plazm* y 16, 1457 (1990).
14. P. Blasi and D. de Marco, *Astropart. Phys.* 20, 559 (2004) [astro-ph/0307067]; M. Kachelrie and D. Semikoz, *Astropart. Phys.* 23, 486 (2005) [astro-ph/0405258].
15. A. Cuoco et al., *Astrophys. J.* 676, 807 (2008) [0709.2712 [astro-ph]].
16. A. Mücke et al., *Comput. Phys. Commun.* 124, 290 (2000) [astro-ph/9903478].
17. V. Berezinsky, A. Z. Gazizov and S. I. Grigor'eva, *Phys. Rev. D* 74, 043005 (2006) [hep-ph/0204357].
18. See also Ref. [17] and V. Berezinsky, A. Gazizov and M. Kachelrie, *Phys. Rev. Lett.* 97, 231101 (2006) [astro-ph/0612247].
19. D. Harari, S. Mollerach and E. Roulet, *JCAP* 0611, 012 (2006) [astro-ph/0609294].
20. O. E. Kalashev et al., arXiv:0710.1382 [astro-ph].
21. V. Berezinsky, A. Z. Gazizov and S. I. Grigor'eva, astro-ph/0210095; *Phys. Lett. B* 612 (2005) 147 [astro-ph/0502550].
22. D. Allard, E. Parizot and A. V. Olinto, *Astropart. Phys.* 27, 61 (2007) [astro-ph/0512345].
23. M. Ave et al., in *Proc. 30th International Cosmic Ray Conference*, Merida, Mexico, 2007, # 0297.